EFFICIENT METHOD FOR COMPUTING WITH CERTAINTY PERIODIC ORBITS ON A SURFACE OF SECTION

E. A. PERDIOS[1], V. S. KALANTONIS[1] and M. N. VRAHATIS[2,3]
[1]*Department of Engineering Sciences, University of Patras, GR–26500 Patras, Greece*
[2]*Department of Mathematics, University of Patras, GR–26500 Patras, Greece*
[3]*University of Patras Artificial Intelligence Research Center (UPAIRC), GR–26500 Patras, Greeces*

(Received: 10 April 2001; accepted: 27 February 2002)

Abstract. We present an improved method for locating periodic orbits of a dynamical system of arbitrary dimension. The method first employs the characteristic bisection method (CBM) to roughly locate a periodic orbit, followed by the quadratically convergent Newton method to rapidly refine its position. The method is applied to the physically interesting example of the two degrees of freedom photogravitational problem, and shown to surpass the CBM algorithm and Newton's method alone.

Keywords: periodic orbits, Poincaré map, surface of section, dynamical systems photogravitational problem, fixed points, zeros of functions, topological degree, Newtons method, characteristic bisection method, generalized bisection method

1. Introduction

In the effort to understand the structure of the solutions of a non-integrable dynamical system, numerical determination of its periodic solutions and their stability properties plays a role of fundamental importance. The fact that for most dynamical systems the periodic orbits are dense in the set of all possible solutions, at least in certain parts of the phase space, necessitates the presence of an efficient numerical method for their determination. Traditional iterative schemes such as Newton's method and related classes of algorithms often fail to converge to a specific periodic solution, since their convergence depends strongly on the initial guess, while there exist several solutions close to each other.

In this paper we propose an efficient method for the rapid computation of a periodic orbit with certainty. First, the method utilizes the *characteristic bisection* (CHABIS) method, which exploits the topological degree theory to locate a periodic orbit within relatively large regions of initial conditions (Vrahatis, 1988, 1995). Then, when the orbit is located with modest accuracy, sufficient for the location to be used as initial guess so that the conditions of convergence of Newton's method are satisfied, the method computes the orbit utilizing *Newton's method*. Our approach is based on the Poincaré map Φ on a surface of section. We say that $\mathbf{x} = (x_1, \ldots, x_n)$ is a *fixed point* or a *periodic orbit* of Φ if $\Phi(\mathbf{x}) = \mathbf{x}$ and a *periodic orbit of period* p if:

$$\mathbf{x} = \Phi^p(\mathbf{x}) \equiv \underbrace{\Phi(\Phi(\cdots(\Phi(\mathbf{x}))\cdots))}_{p \text{ times}}. \quad (1)$$

Celestial Mechanics and Dynamical Astronomy **84:** 231–244, 2002.

From the above it is evident that the problem of computing a periodic orbit is equivalent to the problem of evaluating a fixed point of the Poincaré map.

In this paper, we use our approach to compute efficiently and rapidly periodic orbits of the well-known photogravitational restricted circular three-body problem, described by Radzievskii (1950).

The paper is organized as follows. In the next section, we present the proposed method for computing within a given box in the surface of section periodic orbits of a given period. In Section 3, we briefly present the photogravitational problem. In Section 4, we apply the proposed method to the computation of periodic orbits of the photogravitational problem. The paper ends with some concluding remarks.

2. The Proposed Method

In this section, we describe the proposed method (CHABISNEWT), which is based on the characteristic bisection (CHABIS) and Newton's (NEWT) method.

Many problems in different areas of science and technology can be reduced to a study of a set of solutions of a system of nonlinear equations of the form:

$$\mathbf{F}(\mathbf{X}) = \mathbf{0}, \tag{2}$$

in an appropriate space. Topological degree theory has been developed as means of examining this solution set and obtaining information on the existence of solutions, their number and their nature. This theory is widely used in the study of nonlinear differential (ordinary and partial) equations. It is useful, for example, in bifurcation theory and for providing information about the existence and stability of periodic solutions of ordinary differential equations as well as the existence of solutions of certain partial differential equations. Several of these applications involve the use of various fixed point theorems which can be provided by means of topological degree (Cronin, 1964; Lloyd, 1978; Vrahatis, 1989; Vrahatis, 1995; Vrahatis et al., 1996; Vrahatis et al., 1997; Mourrain et al., 2001).

Next, we will briefly discuss the characteristic bisection method based on the characteristic polyhedron concept for the computation of periodic orbits. The problem of finding periodic orbits of period p of dynamical systems in $\mathbb{R}^{n+1}$ amounts to fixing one of the variables, say $x_{n+1} =$ const., and locating points $\mathbf{X}^\star = (x_1^\star, x_2^\star, \dots, x_n^\star)$ on an n-dimensional surface of section Σ_{t_0} which satisfy the equation

$$\Phi^p(\mathbf{X}^\star) = \mathbf{X}^\star, \tag{3}$$

where $\Phi^p = P_{t_0} : \Sigma_{t_0} \to \Sigma_{t_0}$ is the Poincaré map of the system. This is equivalent to solving system (2) with $\mathbf{F} = (f_1, f_2, \dots, f_n) = \Phi^p - I_n$, where I_n is the $n \times n$ identity matrix and $\mathbf{0} = (0, 0, \dots, 0)$ is the origin of $\mathbb{R}^n$. It is well known that if we have a function $\mathbf{F}$, which is continuous in an open and bounded domain $\mathcal{D}$ and the topological degree of $\mathbf{F}$ at $\mathbf{0}$ relative to $\mathcal{D}$ is not equal to zero, then there is at least one solution of system (2) within $\mathcal{D}$. This criterion can be used, in combination with the construction of a suitable n-polyhedron, called the characteristic polyhedron, for the calculation of a solution contained in this region. This can be done as follows. Let $\mathcal{M}_n$ be the $2^n \times n$ matrix whose rows are formed by all possible combinations of -1 and 1. Consider now an oriented n-polyhedron Π^n, with vertices $\mathbf{V}_k$, $k = 1, \ldots, 2^n$. If the $2^n \times n$ *matrix of signs associated with* $\mathbf{F}$ *and* Π^n, $\mathcal{S}(\mathbf{F}; \Pi^n)$, whose entries are the vectors

$$\operatorname{sgn} \mathbf{F}(\mathbf{V}_k) = (\operatorname{sgn} f_1(\mathbf{V}_k), \operatorname{sgn} f_2(\mathbf{V}_k), \ldots, \operatorname{sgn} f_n(\mathbf{V}_k)), \tag{4}$$

(where sgn denotes the well known three valued sign function), is identical to $\mathcal{M}_n$, possibly after some permutations of these rows, then Π^n is called the *characteristic polyhedron relative to* $\mathbf{F}$. Furthermore, if $\mathbf{F}$ is continuous, then, under some suitable assumptions on the boundary of Π^n,

$$\deg[\mathbf{F}, \Pi^n, \mathbf{0}] = \sum_{\mathbf{X} \in \mathbf{F}^{-1}(\mathbf{0}) \cap \mathring{\Pi}^n} \operatorname{sgn} \det J_{\mathbf{F}}(\mathbf{X}) = \pm 1 \neq 0, \tag{5}$$

where $\deg[\mathbf{F}, \Pi^n, \mathbf{0}]$ denotes the topological degree of $\mathbf{F}$ at $\mathbf{0}$ relative to Π^n, $\mathring{\Pi}^n$ determines the interior of Π^n and $\det J_{\mathbf{F}}(\mathbf{X})$ denotes the determinant of the Jacobian matrix at $\mathbf{X}$), which implies the existence of a periodic orbit inside Π^n.

To clarify the characteristic polyhedron concept we consider a function $\mathbf{F} = (f_1, f_2)$. Each function f_i, $i = 1, 2$, separates the space into a number of different regions, according to its sign, for some regions $f_i < 0$ and for the rest $f_i > 0$, $i = 1, 2$. Thus, in Figure 1(a) we distinguish between the regions where $f_1 < 0$ and $f_2 < 0$, $f_1 < 0$ and $f_2 > 0$, $f_1 > 0$ and $f_2 > 0$, $f_1 > 0$ and $f_2 < 0$. Clearly, the following combinations of signs are possible; $(-, -)$, $(-, +)$, $(+, +)$, and $(+, -)$. Picking a point, close to the solution, from each region we construct

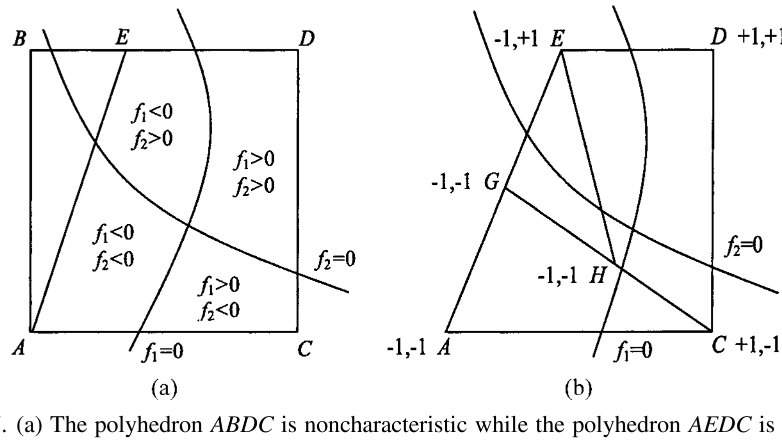

Figure 1. (a) The polyhedron *ABDC* is noncharacteristic while the polyhedron *AEDC* is characteristic. (b) Application of the characteristic bisection method to the characteristic polyhedron *AEDC*, giving rise to the polyhedra *GEDC* and *HEDC*, which are also characteristic.

a characteristic polyhedron. In this figure, we can perceive a characteristic and a noncharacteristic polyedron Π^2. For a polyhedron Π^2 to be characteristic all the above combinations of signs must appear at its vertices. Based on this criterion, polyhedron *ABDC* does not qualify as a characteristic polyhedron, whereas *AEDC* does.

Next, we describe the *characteristic bisection method*. This method simply amounts to constructing another refined characteristic polyhedron, by bisecting a known one, say Π^n, in order to determine the solution with the desired accuracy. We compute the midpoint $\mathbf{M}$ of a 1-simplex, for example, $\langle \mathbf{V}_i, \mathbf{V}_j \rangle$, which accounts for an one-dimensional edge of Π^n. The endpoints of this one-dimensional line segment are vertices of Π^n, for which the corresponding coordinates of the vectors, $\operatorname{sgn} \mathbf{F}(\mathbf{V}_i)$ and $\operatorname{sgn} \mathbf{F}(\mathbf{V}_j)$ differ from each other only in one entry. We call this 1-simplex proper 1-simplex. To obtain another characteristic polyhedron Π^n_* we compare the sign of $\mathbf{F}(\mathbf{M})$ with that of $\mathbf{F}(\mathbf{V}_i)$ and $\mathbf{F}(\mathbf{V}_j)$ and substitute $\mathbf{M}$ for that vertex for which the signs are identical. Subsequently, we reapply the aforementioned technique to a different edge (for details we refer to Vrahatis, 1988; Vrahatis, 1995). In particular, let $\langle \mathbf{V}_i, \mathbf{V}_j \rangle$ be a proper 1-simplex of Π^n and let $\mathbf{B} = (\mathbf{V}_i + \mathbf{V}_j)/2$ be its midpoint. We then distinguish the following three cases:

1. If the vectors $\operatorname{sgn} \mathbf{F}(\mathbf{B})$ and $\operatorname{sgn} \mathbf{F}(\mathbf{V}_i)$ are identical $\mathbf{B}$ replaces $\mathbf{V}_i$ and the process continues with the next proper 1-simplex.
2. If the vectors $\operatorname{sgn} \mathbf{F}(\mathbf{B})$ and $\operatorname{sgn} \mathbf{F}(\mathbf{V}_j)$ are identical then $\mathbf{B}$ replaces $\mathbf{V}_j$ and the process continues with the next proper 1-simplex.
3. Otherwise the process continues with the next proper 1-simplex.

To fully comprehend the characteristic bisection method we illustrate in Figure 1(b), its repetitive operation on a characteristic polyhedron Π^2. Starting from the edge AE we find its midpoint G and then calculate its vector of signs, which is $(-1, -1)$. Thus, vertex G replaces A and the new refined polyhedron $GEDC$, is also characteristic. Applying the same procedure, we further refine the polyhedron by considering the midpoint H of GC and checking the vector of signs at this point. In this case, its vector of signs is $(-1, -1)$, so that vertex G can be replaced by vertex H. Consequently, the new refined polyhedron $HEDC$ is also characteristic. This procedure continues up to the point that the midpoint of the longest diagonal of the refined polyhedron approximates the root within a predetermined accuracy.

Consider the characteristic n-polyhedron, Π^n, whose longest edge length is $\Delta(\Pi^n)$. The minimum number ζ of bisections of the edges of Π^n required to obtain a characteristic polyhedron Π^n_* whose longest edge length satisfies $\Delta(\Pi^n_*) \leqslant \varepsilon$, for some accuracy $\varepsilon \in (0, 1)$, is given by

$$\zeta = \left\lceil \log_2(\Delta(\Pi^n)\, \varepsilon^{-1}) \right\rceil . \tag{6}$$

Notice that ζ is independent of the dimension n, implying that the bisection algorithm performs the same number of iterations as the bisection in one-dimension, which is optimal and asymptotically possesses the best rate of convergence

(Sikorski, 1982). The characteristic bisection method is efficient for low dimensions (say, $n \leqslant 10$). This is due to the fact that the starting box as well as the characteristic polyhedron require 2^n vertices.

The characteristic bisection method has been applied to numerous difficult problems (see e.g. Drossos et al., 1996; Waalkens et al., 1997; Burić and Mudrinić, 1998; Kalantonis et al., 2001; Vrahatis et al., 2001). The characteristic bisection method is very useful in cases where the period of the periodic orbit is very high and especially when the orbit is unstable, since the method always converges within the initial specified region. Although this method computes a specific periodic orbit with certainty, its convergence is not as rapid as that of Newton's method, which is known to be quadratic.

With the proposed method CHABISNEWT we improve the computational speed of the characteristic bisection method by combining it with Newton's method. This is achieved as follows. First the characteristic bisection method locates the periodic solution. Once the solution is located with a predetermined modest accuracy (2 to 3 decimal digits), sufficient for the conditions of convergence of Newton's method to be satisfied, we proceed to employ Newton's method to compute the orbit with full accuracy and quadratic convergence.

A periodic orbit can be determined by Newton's method as follows: If $(x_0, \dot{x}_0)$ are the initial conditions of an orbit at $t_0 = 0$, on the surface of section of the Poincaré map for a certain value of the Jacobian constant C, then the periodicity conditions that must be satisfied are:

$$x(x_0, \dot{x}_0) = x_0, \qquad \dot{x}(x_0, \dot{x}_0) = \dot{x}_0. \tag{7}$$

Since these are not satisfied for an initial guess $(x_0, \dot{x}_0)$ we consider corrections δx_0 and $\delta \dot{x}_0$ such that:

$$\begin{aligned} x(x_0 + \delta x_0, \dot{x}_0 + \delta \dot{x}_0) &= x_0 + \delta x_0, \\ \dot{x}(x_0 + \delta x_0, \dot{x}_0 + \delta \dot{x}_0) &= \dot{x}_0 + \delta \dot{x}_0. \end{aligned} \tag{8}$$

Expanding to first-order terms in the corrections, we obtain the corrector system:

$$\begin{aligned} &\left(\frac{\partial x}{\partial x_0} - 1\right)\delta x_0 + \frac{\partial x}{\partial \dot{x}_0}\delta \dot{x}_0 = x_0 - x, \\ &\frac{\partial \dot{x}}{\partial x_0}\delta x_0 + \left(\frac{\partial \dot{x}}{\partial \dot{x}_0} - 1\right)\delta \dot{x}_0 = \dot{x}_0 - \dot{x}. \end{aligned}$$

It is important here to recognize that the derivatives involved refer to isoenergetic variations in accordance with the definition of the mapping of the Poincaré surface of section into itself. We then write the above corrector in the form:

$$\begin{aligned} &(a - 1)\delta x_0 + b\delta \dot{x}_0 = x_0 - x, \\ &c\delta x_0 + (d - 1)\,\delta \dot{x}_0 = \dot{x}_0 - \dot{x}, \end{aligned} \tag{9}$$

where $a = \partial x/\partial x_0, b = \partial x/\partial \dot{x}_0, c = \partial \dot{x}/\partial x_0$, and $d = \partial \dot{x}/\partial \dot{x}_0$ are the isoenergetic stability indices of the mapping (Hénon, 1973). The stability indices a, b, c, and d can be obtained with additional integrations but in this application we need high accuracy and so we choose to compute them by integrating the equations of motion simultaneously with the equations of variation and using the formulae of Markellos (1976):

$$
\begin{aligned}
a &= \frac{\partial x_1}{\partial x_{01}} + \frac{\partial x_1}{\partial x_{04}} D_1^4 + D_3^4 \left(\frac{\partial x_2}{\partial x_{01}} + \frac{\partial x_2}{\partial x_{04}} D_1^4 \right), \\
b &= \frac{\partial x_1}{\partial x_{03}} + \frac{\partial x_1}{\partial x_{04}} D_3^4 + D_3^4 \left(\frac{\partial x_2}{\partial x_{03}} + \frac{\partial x_2}{\partial x_{04}} D_3^4 \right), \\
c &= \frac{\partial x_3}{\partial x_{01}} + \frac{\partial x_3}{\partial x_{04}} D_1^4 - \frac{f_{10}}{x_{04}} \left(\frac{\partial x_2}{\partial x_{01}} + \frac{\partial x_2}{\partial x_{04}} D_1^4 \right), \\
d &= \frac{\partial x_3}{\partial x_{03}} + \frac{\partial x_3}{\partial x_{04}} D_3^4 - \frac{f_{10}}{x_{04}} \left(\frac{\partial x_2}{\partial x_{03}} + \frac{\partial x_2}{\partial x_{04}} D_3^4 \right),
\end{aligned} \tag{10}
$$

where

$$
f_{10} = f_1(t = 0), \qquad D_1^4 = \frac{1}{2x_{04}} \frac{\partial F}{\partial x_{01}}, \qquad D_3^4 = -\frac{x_{03}}{x_{04}}.
$$

In this manner the indices a, b, c, d are computed with the accuracy of the numerical integration. The corrector is applied successively until the periodicity conditions are satisfied with the desired accuracy. Newton's method converges rapidly but often needs a very good initial guess. In our proposed scheme this is provided by the CHABIS method which is firstly applied until an accuracy sufficient for the conditions of convergence of Newton's method to be satisfied is achieved.

3. The Photogravitational Problem

Let us briefly describe the photogravitational restricted three-body problem (Radzievskii, 1950). The system of equations that expresses the motion of the third particle is the following:

$$
\begin{aligned}
\ddot{x} &= 2\dot{y} + \frac{\partial \Omega}{\partial x} = f_1, \\
\ddot{y} &= -2\dot{x} + \frac{\partial \Omega}{\partial y} = f_2,
\end{aligned} \tag{11}
$$

where

$$
\begin{aligned}
\Omega &= \frac{1}{2}(x^2 + y^2) + \frac{q_1(1-\mu)}{r_1} + \frac{q_2\mu}{r_2}, \qquad \mu = \frac{m_2}{m_1 + m_2}, \\
r_1 &= \sqrt{(x+\mu)^2 + y^2}, \qquad r_2 = \sqrt{(x+\mu-1)^2 + y^2},
\end{aligned}
$$

while $(1-\mu)$, μ represent the masses of the two main bodies with $\mu \leqslant 0.5$ and q_1, q_2 are parameters expressing the relations between the gravitation attraction and the radiation pressure of each one of them, $q_i \leqslant 1$, $i = 1, 2$. The Jacobian integral of the above system is given by the following equation:

$$F(x, y, \dot{x}, \dot{y}) = (\dot{x}^2 + \dot{y}^2) - 2\Omega = C, \tag{12}$$

where C is the Jacobi ('energy') constant.

4. Numerical Results

We apply the proposed method to the restricted circular photogravitational three-body problem described by Equations (11), for particular values of the parameters $q_1 = 0.5$, $q_2 = 1$, and $\mu = 0.01214$. To produce the surface of section of the problem, we take successive sections of an orbit with the straight line $y = 0$, along the positive direction of the flow ($\dot{y} > 0$). Thus, the initial conditions are $(x, 0, \dot{x}, \dot{y})$ where the value of $\dot{y}$ is computed using Equation (12) for a given value of C. A periodic orbit of period p intersects the x-axis $2p$ times and thereupon a p periodic orbit is represented by p points in $(x, \dot{x})$ plane. To compute successively the intersection points with the surface of section, we choose a value of the Jacobian constant C and by keeping this value fixed we integrate numerically Equations (11) (for details see Kalantonis et al., 2001). An example of a surface of section is shown in Figures 2(a), (b) (for arbitrarily chosen Jacobian constant $C_{L_2} = -2.31058003$).

For the specific surfaces of section shown in Kalantonis et al. (2001), we apply and compare the methods described in Section 2 to the computation of periodic orbits of the photogravitational problem with accuracy $\varepsilon \leqslant 10^{-8}$.

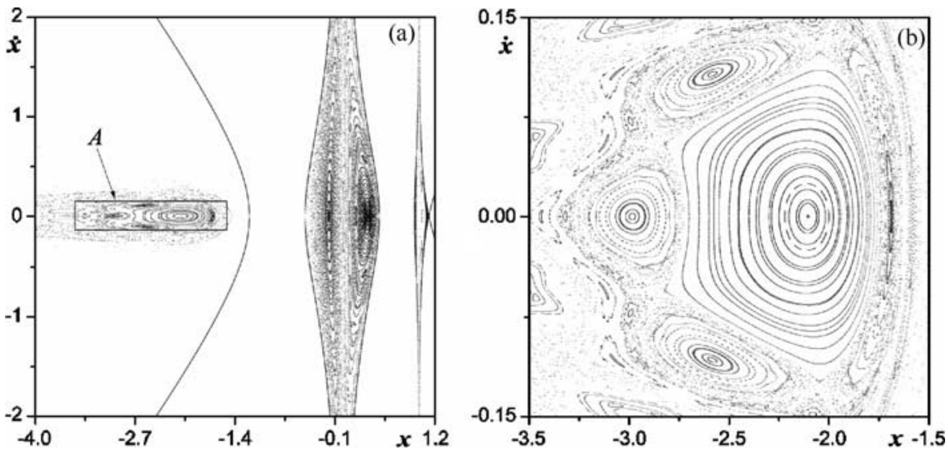

Figure 2. (a) Surface of section points and the invariant curves of system 11 with parameters $q_1 = 0.5$, $q_2 = 1$, and $\mu = 0.01214$, for $C_{L_2} = -2.31058003$, (b) magnification of box A.

We find that the method of the characteristic polyhedron always converges to the periodic solution (within any region that does not contain orbits whose period is a sub-multiple of the period of the desired orbit). This means that the method of the characteristic polyhedron can converge equally well to stable as well as to unstable periodic orbits, independently of the initial guess.

A further advantage of the characteristic bisection method is the ease with which we can distinguish the exact location of all periodic orbits of a given period, including the unstable orbits. This can be achieved through the coloring of the surface of the section. The coloring process works as follows. Suppose that the periodic orbit under consideration is of period p. Denote the initial point by $(x_0, \dot{x}_0)$. We integrate the equations of motion, starting from $(x_0, \dot{x}_0)$, up to the point that the orbit intersects the x-axis $2p$ times. Let $(x, \dot{x})$ denote the point at the end of the integration. We evaluate the signs of the following differences:

$$(x - x_0) \quad \text{and} \quad (\dot{x} - \dot{x}_0). \tag{13}$$

Clearly, four combinations of signs are possible; namely $(-,-)$, $(-,+)$, $(+,+)$, and $(+,-)$. Each one of these combinations corresponds to a different color. More specifically, we color white the area that corresponds to the sign combination $(-,-)$, gray for $(-,+)$, light gray for $(+,+)$, and finally dark gray for $(+,-)$. To color the whole plane we select each point contained in the plane as the initial point and apply the coloring procedure. At each point where the four different colors meet, a periodic orbit (stable or unstable) exists.

Examples of the coloring procedure are exhibited in Figures 3(a), (b). These figures correspond to the coloring of the Poincaré surface of section of Figure 2(b). In Figure 3(a) the coloring procedure was applied to detect a 1-period periodic

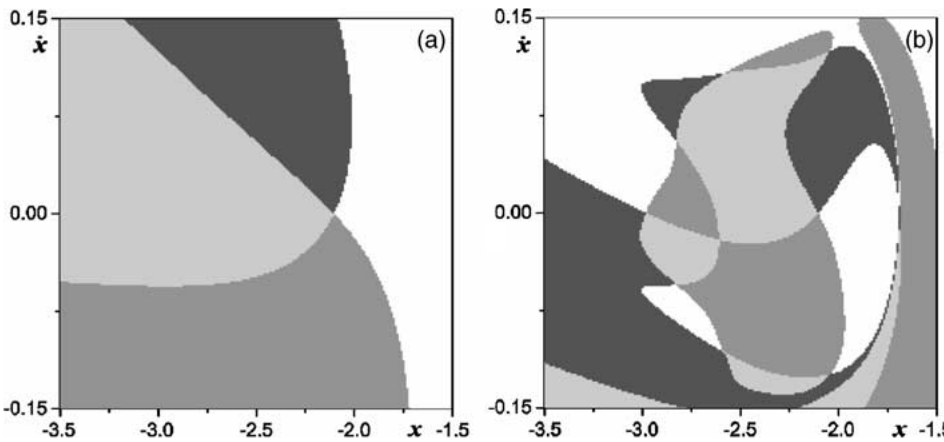

Figure 3. Coloring the $(x, \dot{x})$ plane of system 11 with parameters $q_1 = 0.5$, $q_2 = 1$, and $\mu = 0.01214$, for $C_{L_2} = -2.31058003$. The white color corresponds to the sign combination $(-,-)$, the gray to $(-,+)$, the light gray to $(+,+)$, and the dark gray to $(+,-)$. (a) Locating a 1-period periodic orbit, (b) locating a 4-period periodic orbit.

orbit, whereas in Figure 3(b) a 4-period periodic orbit was detected. In the later figure the 1-period periodic orbit appears due to the fact that its period is a sub-multiple of the period of the 4-period orbit.

In Figures 4(a)–(d) the application of the characteristic bisection method to the photogravitational problem is illustrated. Starting with a polyhedron *ABDC*, Figure 4(a), we examine whether it is characteristic or not. In the particular case *ABDC* is not characteristic; this is easily verifiable by the fact that two vertices of the box have the same color. To overcome this problem, we need to determine a new vertex that will contain the missing combination; such a vertex is E. Having constructed a characteristic polyhedron we legitimately apply the method. In Figure 4(b) we select the midpoint, F, of the largest edge, namely EC, and examine the corresponding combination of signs at F. Since the combination at F is identical to that in C (these two points have the same color), F substitutes C giving rise to a new refined characteristic polyhedron, *ABEF*. Figures 4(c), (d) exhibit two subsequent iterations of this method. Both *GBEF* and *GHEF* are characteristic. Following this procedure the desired solution is successfully captured.

Note that the application of the characteristic bisection method does not require the coloring procedure. We utilized this procedure to illustrate the operation of the method and to provide a visualization of the solution.

Newton's method behaves quite differently, its convergence depending strongly on the initial guess. We have found that the higher the period the smaller are the regions of convergence (a smaller part of the region that does not contain orbits whose period is a sub-multiple of the period of the desired orbit). Thus, for periodic orbits of large period, it turns out that Newton's method needs an initial guess lying within a very small distance from the solution. Figure 5 exhibits examples of the basins of convergence of Newton's method. We observe that the convergence properties of Newton's method, depend on the multiplicity and the stability of the periodic orbit. In Figure 6, we illustrate the typical performance of CHABIS and Newton's method. The basin of convergence of Newton's method for the particular 36-period unstable periodic point is a small irregular area around it. On the other hand CHABIS encloses a large region around the specific periodic point which is determined by any box that does not contain another periodic point of a sub-multiple or the same period.

A comparison of the three methods, namely CHABIS, Newton and CHABIS-NEWT, is shown in Table I. First, we compute the periodic points of Table I using CHABIS. We start with a box surrounding the fixed point (see box A of Figure 6) and refine this box with CHABIS until the desired periodic point $(x, \dot{x})$ of period p is found with accuracy $\varepsilon \leqslant 10^{-8}$. The elapsed CPU time (integral part of seconds) required for this computation is given as t_1 in the table. Next, we have taken the same starting boxes and used the centers of these boxes as initial guesses for Newton's method. The corresponding elapsed CPU time, for the convergence to the same fixed points $(x, \dot{x})$, is given as t_2. Note that for these starting values Newton's

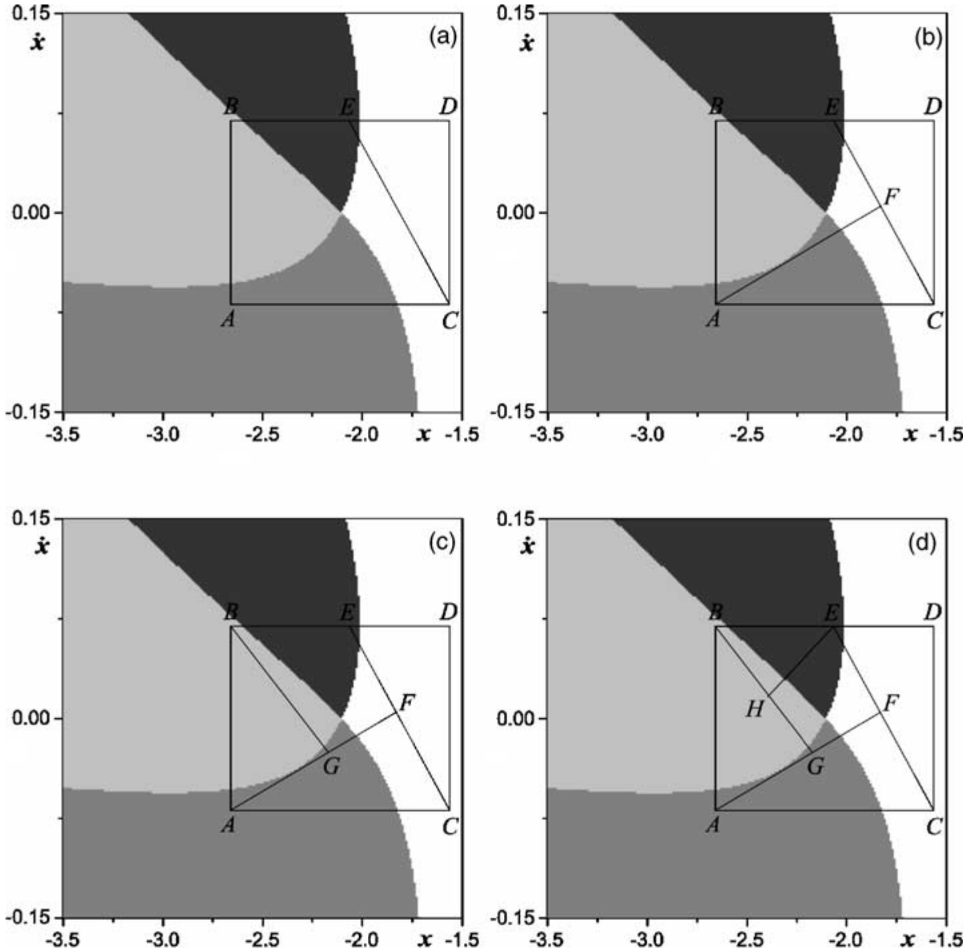

Figure 4. Application of the characteristic bisection method to the photogravitational problem with parameters $q_1 = 0.5$, $q_2 = 1$, and $\mu = 0.01214$, for $C_{L_2} = -2.31058003$. The white color corresponds to the sign combination $(-, -)$, the gray to $(-, +)$, the light gray to $(+, +)$, and the dark gray to $(+, -)$.

method has a rapid convergence to the specific fixed points. But in many cases and in particular for high period points, Newton's method does not converge. In our new approach CHABISNEWT we have combined the advantages of CHABIS and Newton's method. This is evident in Table I since we have succeeded to compute all the periodic orbits as CHABIS has done, but at the same time the convergence was more rapid. An interesting fact is that in some cases CHABISNEWT is faster even than Newton. This is due to the fact that in these cases Newton's method did not converge monotonically.

With CHABISNEWT method we first start with CHABIS in order to compute a periodic point with a modest accuracy, say $\varepsilon \leqslant 10^{-2}$. Then we utilize the obtained

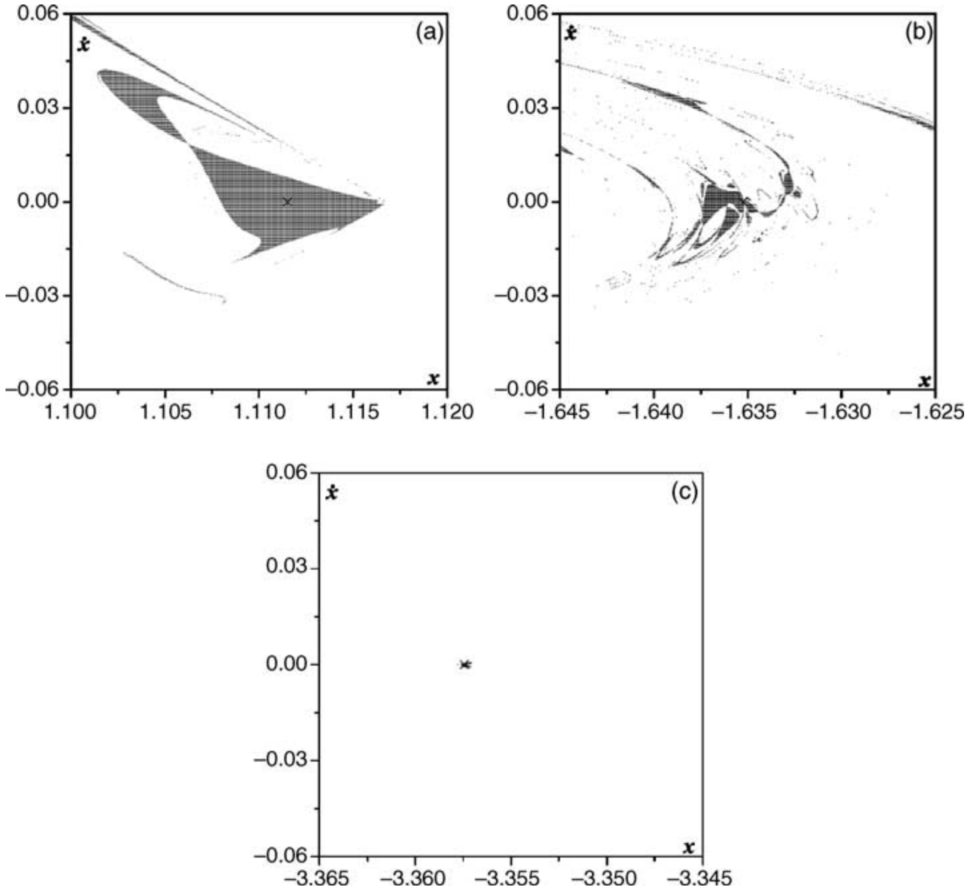

Figure 5. Basins of convergence of Newton's method. The exact position of the periodic points is marked by $\times$. (a) 1-period stable periodic point. (b) 13-period unstable periodic point. (c) 140-period unstable periodic point.

estimate of the orbit as a starting value for Newton's method. If, after one iteration of Newton's method a better approximation is not obtained we apply again CHABIS method using the final characteristic polyhedron obtained by the previous CHABIS application, in order to obtain a more accurate estimate, say $\varepsilon \leqslant 10^{-3}$. Then we apply again Newton's method and so on. For the results exhibited in Table I we have obtained convergence of Newton's method in the CHABISNEWT procedure for almost all cases when CHABIS applied with accuracy $\varepsilon \leqslant 10^{-2}$. But in some cases, such as the two cases of period 140 of Table I, the required accuracy using CHABIS was $\varepsilon \leqslant 10^{-4}$. Also, a surprising result was from a small period point $(x, \dot{x}) = (0.46640390, 0)$ of period 7 where the required accuracy using CHABIS was $\varepsilon \leqslant 10^{-4}$.

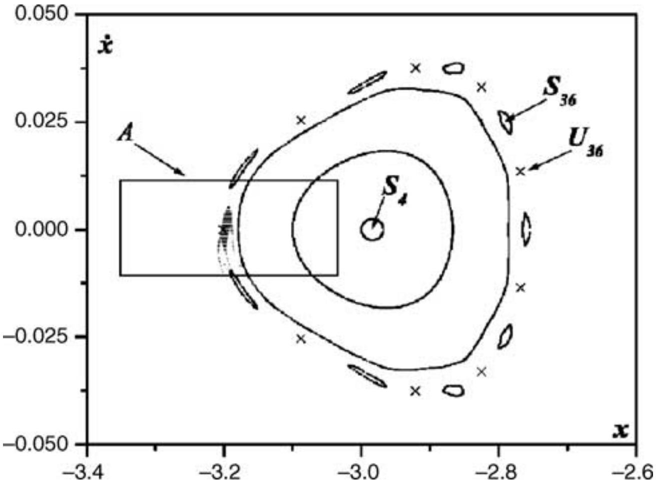

Figure 6. A typical example showing the convergence properties of the CHABIS and Newton methods. The irregular gray area within box A represents the basin of convergence of Newton's method while the box A represents the basin of convergence of CHABIS. S_4 indicates a 4-period stable periodic orbit, S_{36} indicates a 36-period stable periodic orbit, and U_{36} indicates a 36-period unstable periodic orbit.

TABLE I

Fixed points of periodic orbits of period p on the Poincaré surface of section for system (11) using Jacobian constant $C_{L_2} = -2.31058003$; CPU time t in seconds (integral part) required for their computation within accuracy $\varepsilon \leqslant 10^{-8}$ the method of CHABIS (t_1), Newton's method (t_2) and the proposed method CHABISNEWT (t_3); NC indicates non-convergence; symmetry identification *Sym.* ('*S*' denotes symmetry while 'A' denotes asymmetry)

p	Fixed point $(x, \dot{x})$	t_1	t_2	t_3	*Sym.*
1	(0.93717344, 0.00000000)	1	0	0	*S*
1	(1.11150338, 0.00000000)	1	0	0	*S*
1	(−2.10504200, 0.00000000)	1	0	0	*S*
1	(−0.18431881, 0.00000000)	1	0	0	*S*
1	(0.32311727, 0.00000000)	1	0	0	*S*
3	(0.16581940, 0.00000000)	3	0	0	*S*
3	(0.43782960, 0.00000000)	2	2	1	*S*
4	(−2.98416804, 0.00000000)	1	1	1	*S*
4	(−2.82606292, 0.05524204)	2	1	1	*A*
5	(−1.57785783, 0.00000000)	2	1	1	*S*
5	(−3.65008738, 0.00000000)	2	1	1	*S*
7	(−2.47322591, 0.00000000)	3	1	1	*S*
7	(−1.84329896, 0.00000000)	4	NC	1	*S*
7	(0.09075069, 0.00000000)	8	2	1	*S*

TABLE I
(*continued*)

p	Fixed point $(x, \dot{x})$	t_1	t_2	t_3	*Sym.*
7	(0.46640390, 0.00000000)	7	NC	4	S
9	(−3.44436456, 0.00000000)	6	1	1	S
9	(−1.62423304, 0.00000000)	5	1	1	S
11	(−2.62914789, 0.00000000)	5	3	1	S
11	(−1.78051126, 0.00000000)	5	2	2	S
13	(−3.32141447, 0.00000000)	5	1	2	S
13	(−1.63525729, 0.00000000)	8	NC	2	S
17	(−3.27000405, 0.00000000)	6	4	3	S
17	(−1.64026111, 0.00000000)	8	NC	5	S
19	(−2.71020057, 0.00000000)	12	4	3	S
19	(−1.75442473, 0.00000000)	13	9	6	S
22	(−3.36990585, 0.00000000)	6	5	4	S
22	(−3.05346495, −0.07823604)	13	4	6	A
23	(−2.71984195, 0.00000000)	11	3	3	S
23	(−1.75154707, 0.00000000)	19	NC	7	S
25	(−1.59026031, 0.00000000)	11	3	3	S
25	(−1.56733859, 0.00000000)	12	NC	3	S
32	(−1.72895845, 0.00000000)	13	NC	4	S
32	(−3.16205619, 0.00000000)	14	8	6	S
35	(−3.35824891, 0.00000000)	9	NC	3	S
35	(−1.63329154, 0.00000000)	15	NC	8	S
36	(−2.75989136, 0.00000000)	18	NC	5	S
36	(−3.20216680, 0.00000000)	18	NC	9	S
52	(−2.99324919, 0.06747215)	20	NC	6	A
52	(−3.33276884, 0.00000000)	20	NC	11	S
140	(−3.03248329, 0.05557997)	63	NC	29	A
140	(−3.35744012, 0.00000000)	85	NC	29	S

5. Epilogue

In this paper, we have proposed a composite method for computing efficiently and with certainty periodic orbits on a surface of section of the Poincaré map. We have applied this method to compute periodic orbits of the photogravitational restricted circular three-body problem.

The proposed method utilizes the characteristic bisection and Newton's method, combining the advantages of both methods. First, it utilizes the characteristic bisection method, within a box around a periodic point of a given period, to locate it with certainty. When the solution is located with a predetermined modest accuracy sufficient for the conditions of convergence of Newton's method to be satisfied, the method utilizes Newton's method, with accurately computed stability indices of the Poincaré map, to compute the orbit with quadratic convergence. The proposed method computes all the solutions efficiently.

Acknowledgements

We would like to thank Prof. V. V. Markellos for his useful suggestions. We also wish to thank the referees for their useful comments. During this work V. S. Kalantonis was the recipient of the 'K. Karatheodoris' research grant.

References

Burić, N. and Mudrinić, M.: 1998, *J. Phys. A: Math. Gen.* **31**, 1875.
Cronin, J.: 1964, *Fixed Points and Topological Degree in Nonlinear Analysis*, Mathematical Surveys No. 11, Amer. Math. Soc., Providence, Rhode Island.
Drossos, L., Ragos, O., Vrahatis, M. N. and Bountis, T. C.: 1996, *Phys. Rev. E* **53** (1), 1206.
Hénon, M.: 1973, *Astron. Astrophys.* **28**, 415.
Kalantonis, V. S., Perdios, E. A., Perdiou, A. E. and Vrahatis, M. N.: 2001, *Celest. Mech. & Dyn. Astr.* **80**, 81.
Lloyd, N. G.: 1978, *Degree Theory*, Cambridge University Press, Cambridge.
Markellos, V. V.: 1976, *Astrophys. Space Sci.* **43**, 449.
Mourrain, B., Vrahatis, M. N. and Yakoubsohn, J. C.: 2001, *J. Complex.* (accepted for publication).
Radzievskii, V. V.: 1950, *Astron. Zh.* **27**, 250.
Sikorski, K.: 1982, *Numer. Math.* **40**, 111.
Vrahatis, M. N.: 1988, *ACM Trans. Math. Softw.* **14**, 312; ibid **14**, 330.
Vrahatis, M. N.: 1989, *Proc. Amer. Math. Soc.* **107**, 701.
Vrahatis, M. N.: 1995, *J. Comp. Phys.* **119**, 105.
Vrahatis, M. N., Bountis, T. C. and Kollmann, M.: 1996, *Inter. J. Bifurc. Chaos* **6**, 1425.
Vrahatis, M. N, Isliker, H. and Bountis, T. C.: 1997, *Inter. J. Bifurc. Chaos* **7**, 2707.
Vrahatis, M. N., Perdiou, A. E., Kalantonis, V. S., Perdios, E. A., Papadakis, K., Prosmiti, R. and Farantos, S. C.: 2001, *Comput. Phys. Commun.* **138**, 53.
Waalkens, H., Wiersig, J. and Dullin, H. R.: 1997, *Ann. Phys.* **260**, 50.